Journal of ELECTRICAL ENGINEERING, VOL. 58, NO. 2, 2007, 71–78

NEW EXTENDED CASCADED PREDICTIVE CONTROL WITH MULTIPLE REFERENCE MODELS ECGPC/MRM OF AN INDUCTION MOTOR DRIVE WITH EFFICIENCY OPTIMIZATION

Kamel Barra [*] — **Khier Benmahammed** [**]

In this paper, a new extended cascaded predictive control with multiple reference models method ECGPC/MRM is synthesized under energy saving control of an induction motor drive to improve high efficiency of the drive system. The method gives the possibility to control at the same time different variables more than in conventional CGPC. For this method, the plant is assumed to be divided into three parts and three G.P.C algorithms must be computed. The control law is then derived under polynomial structure in order to analyze the stability of the different controlled open loops in the frequency domain. Simulation results demonstrate the performance of the proposed method.

K e y w o r d s: induction motor, cascaded generalized predictive control, energy saving control

1 INTRODUCTION

Induction motors are receiving wide attention in industrial applications due to their large speed capability, mechanical robustness, cheapness and ease of maintenance [1–9]. It has been shown in previous studies [1, 2] that electrical machines consume about 60 % of the total consumed electrical energy, thereof integral horse power induction motors account for 96 % of the energy consumption. This means that around 56 % of the total electrical energy is consumed by induction motors. Also about 70 % of the energy loss is dissipated in motors with a rating below 52 kW, consequently, the tendency is to concentrate the energy saving studies on induction motor drives below 52 kW rated power.

The key to solving the energy saving problem in induction motors is to obtain the better balance between different types of motor losses. Recently, many studies on efficiency maximization techniques have been presented and they may be divided into two categories [3, 6]: Loss model controller (LMC) and Search controller (SC). Both methods minimized the motor losses but in different ways. The LMC method calculates the optimum of the objective function (which is an analytical expression representing the total losses of the machine). The fast determination of the optimum variables is the merit of this method, but it is sensitive to parameter variations. Hence, if the LMC approach is not based on an on-line estimation of the parameters, then it is likely that the method may offer only sub-optimal solution if the parameters of the machine change (due to saturation, temperature variations, skin effect, *etc*). The SC technique depends on the exact measurement of the input power and converges slowly to the true optimum variables. The advantage of this approach is independence of parameter variations. However, some disadvantages appear in practice, such as continuous disturbance in the torque caused by stepwise changes of the control variable, slow convergence, because it has no idea about the optimal magnitude of variables at the beginning of search process, difficulties in tuning the algorithm for a given application and inaccuracy in efficiency optimization. For these reasons, this is not a good method in industrial drives.

An exhaustive analysis of the LMC controller can be found in the literature [1–11]. In [3], the authors calculated the total power loss of the induction motor only (the inverter loss is not taken into account) and derived an optimal flux level that maximizes the motor efficiency. In [8], a simple model neglecting the leakage inductance has been presented and the motor model consists only of resistors reflecting core loss, rotor and stator copper losses as a function of stator current components, then, a d-axis current level is derived that minimizes the total loss. Consequently, exact loss minimization can not be achieved, especially for high speed operation (especially in the area of electrical vehicles). The authors in [9] used copper and core loss only to formulate the cost function of motor loss and adjusted the optimal rotor flux under state constraints of the inverter. Note that none of the studies described previously attempts to account for the inverter loss in the global cost function of total loss.

Over the last decade, generalized predictive control GPC has received an increasing attention in many control applications and it has shown to be an effective strategy for high performance applications compared to some conventional control methods, with good temporal and frequency properties (small overshoot, cancellation of disturbances, good stability and robustness margins) [12–14]. GPC is a model based method which employs receding horizon approach in order to predict future outputs.

[*] Department of Electrical Engineering, University of Larbi Ben M'hidi, Oum El Bouaghi, 04000 Algeria. E-mail: barakamel@yahoo.fr
[**] Department of Electronics, University of Setif, 19000 Algeria.

ISSN 1335-3632

An appropriate sequence of the control signals is then calculated to reduce the tracking error by minimizing a quadratic cost function. After which only the first element of control signals is applied on the system. The process is repeated for every sample of duration, so that new information is updated at each sample interval. Cascaded generalized predictive control CGPC is a method issued from GPC [15–17], which gives the possibility to control conventionally only two different variables together in electrical machines (position and speed). The main interest of a predictive structure with multiple reference models is to ensure an input-output asymptotic behaviour which corresponds to a stable tracking model chosen by the user [17].

The main contribution of this paper is to present a new ECGPC/MRM to control many different variables simultaneously based on an energy saving control needed for high performance induction motor drive capability. The external loop uses a simple GPC controller and the inner loops uses a GPC/MRM with multiple reference models in order to follow specified trajectories. The remainder of the paper can be outlined as follows: in section 2, a loss minimization algorithm of an induction motor drive including copper loss, core loss, stray load loss and inverter loss is developed to maximize the efficiency of the drive system. Based on that, a relationship which permits to determine the global control signal of the extended cascaded chain is derived. Section 3 describes the extended ECGPC/MRM cascade. Section 4 proposes a method for stability analysis. The simulation results of the system are presented in section 5 which carries out the performance of the drive system. Finally, some conclusions are derived and given in section 6.

2 ENERGY SAVING CONTROL

2.1 Motor loss model

Core loss

The stator core loss due to fundamental frequency mutual flux ϕ (air-gap flux) consists of eddy-current loss and hysteresis loss, and they are given by Steinmetz's formula as

$$P_{cs} = K_e f_s^2 \phi^2 + K_h f_s \phi^2 \,. \tag{1}$$

The corresponding rotor core loss is given as [1, 2]

$$P_{cr} = \frac{m_r}{m_s} \left[K_e (s f_s)^2 \phi^2 + K_h (s f_s) \phi^2 \right], \tag{2}$$

where s denotes the slip, m_s and m_r denote the mass of stator and rotor core, respectively, K_e and K_h are properties of the material. Note that the rotor core loss is quite small compared with the stator core loss, since $g f_s \ll f_s$, then the total core loss of the machine is

$$P_{cl} = P_{cs} + P_{cr} \approx P_{cs} \,. \tag{3}$$

The stator equivalent core loss resistance R_{fs} is determined from the classical experimental no-load test data as [5]

$$R_{fs} = a_1 f_s + a_2 f_s^2, \tag{4}$$

where a_1 and a_2 are the coefficients of hysteresis and eddy-current loss, respectively ($a_1 = 0.0599$, $a_2 = 0.0032$).

Copper loss

Stator copper loss:

$$P_{js} = R_s \left(i_{ds}^2 + i_{qs}^2 \right) \tag{5}$$

Rotor copper loss:
At the steady state we have

$$P_{jr} = R_r \left(i_{dr}^2 + i_{qr}^2 \right) = \frac{R_r}{(1+\sigma_r)^2} i_{qs}^2 \,. \tag{6}$$

Stray load loss

Since the rotor current in a squirrel cage induction motor is not measurable, it is a common practice to express the stray loss as a function of the stator current by inclusion of an equivalent stray loss resistance R_{st} in series with the stator phase resistance:

$$P_{st} = \left(a_3 f_s + a_4 f_s^2 \right) i_s^2 = R_{st} i_s^2 \,. \tag{7}$$

Here a_3 and a_4 are the stray load loss constants determined from load tests ($a_3 = 0.0042$, $a_4 = 0.0027$) as it is explained by the IEEE standard 112 B method [10].

2.2 Induction motor model

A squirrel cage induction motor model used under field oriented control FOC which tackles more accurately the behaviour of the machine such as stray load resistance and core loss resistance can be expressed in the synchronously rotating d-q reference frame as follows [5]:

$$\begin{aligned}
V_{ds} &= \Big(R_s + R_{st} + \frac{\sigma_r R_{fs}}{1+\sigma_r} \Big) i_{ds} + \sigma L_s \frac{\mathrm{d}i_{ds}}{\mathrm{d}t} \\
&\quad - \sigma L_s \omega_s i_{qs} + \frac{(1-\sigma) L_s}{L_m} \frac{\mathrm{d}\phi_{dr}}{\mathrm{d}t} + \frac{R_{fs}}{L_m (1+\sigma_r)} \phi_{dr}, \\
V_{qs} &= \Big(R_s + R_{st} + \frac{\sigma_r R_{fs}}{1+\sigma_r} \Big) i_{qs} + \sigma L_s \frac{\mathrm{d}i_{qs}}{\mathrm{d}t} \\
&\quad + \sigma L_s \omega_s i_{ds} + \frac{(1-\sigma) L_s \omega_s}{L_m} \phi_{dr} \,, \\
T &= \frac{p L_m}{L_r} \phi_{dr} i_{qs} \,, \quad k_1 = \frac{p L_m}{L_r}
\end{aligned} \tag{8}$$

where $\sigma_s = \frac{l_s}{L_m}$, $\sigma_r = \frac{l_r}{L_m}$, $\sigma = 1 - \frac{L_m^2}{L_s L_r}$,
X_{ds}, X_{qs}: d- and q- axes stator voltages, currents or flux, ω_s, ω_r: synchronous and rotor speed.

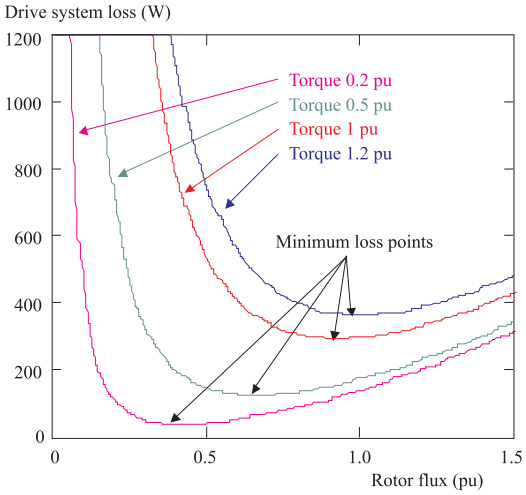

Fig. 1. Total power loss versus rotor flux.

2.3 Inverter loss model

None of the efficiency optimization techniques described recently attempts to account for the inverter loss model in the cost function of total loss. The inverter loss calculation is based on measurement of the diode and transistor conduction voltages and on measurements of the following switching energies: Diode turn-off, transistor turn-on and transistor turn-off. The approximate inverter loss as a function of stator current is given by [7]

$$W_{inv} = a_6\left(i_{ds}^2 + i_{qs}^2\right) + a_7\sqrt{i_{ds}^2 + i_{qs}^2}\,, \tag{9}$$

where a_6 and a_7 are coefficients determined by the electrical characteristics of a switching element. ($a_6 = 0.76$, $a_7 = 5.8$).

2.4 Loss minimization strategy

Power loss W_{tot} of the drive system can be expressed as:

$$\begin{aligned} W_{tot} &= W_{mot} + W_{inv}\,, \\ W_{mot} &= P_{js} + P_{jr} + P_{fs} + P_{st}\,. \end{aligned} \tag{10}$$

Here, mechanical losses are not considered, then, the total power loss of the drive system as a quadratic function of stator current components can be expressed as:

$$W_{tot} = A(\omega_s)i_{ds}^2 + B(\omega_s)i_{qs}^2 + C\sqrt{i_{ds}^2 + i_{qs}^2}\,, \tag{11}$$

where

$$\begin{aligned} A(\omega_s) &= \left(R_s + R_{st}(\omega_s) + R_{fs}(\omega_s) + a_6\right), \\ B(\omega_s) &= \left(R_s + R_{st}(\omega_s) + a_6 + \frac{\sigma_r R_{fs}(\omega_s)}{1+\sigma_r} + \frac{R_r(f_r)}{(1+\sigma_r)^2}\right) \\ C &= a_7\,, \quad k = p\frac{L_m^2}{L_r}\,. \end{aligned} \tag{12}$$

Also, the total power loss of the drive system W_{tot} can be expressed as a function of torque and rotor flux as

$$W_{tot} = \frac{A(\omega_s)}{L_m^2}\phi_r^2 + B(\omega_s)\left(\frac{L_m}{k}\right)^2\left(\frac{T}{\phi_r}\right)^2 + C\sqrt{\left(\frac{\phi_r}{k}\right)^2 + \left(\frac{L_m}{k}\right)^2\left(\frac{T}{\phi_r}\right)^2}\,. \tag{13}$$

Figure 1 shows the plot of the total power loss of the drive system W_{tot} including the inverter loss at a constant speed ($f_s = 50$ Hz) versus rotor flux for different load torques.

2.5 Optimal solution

The steady state electromagnetic torque is given by

$$T = p\frac{L_m^2}{L_r}i_{qs}i_{ds} = ki_{qs}i_{ds}\,. \tag{14}$$

We consider the following problem: Minimize

$$W_{tot} = A(\omega_s)i_{ds}^2 + B(\omega_s)i_{qs}^2 + C\sqrt{i_{ds}^2 + i_{qs}^2} \tag{15}$$

subject to the equality constraint:

$$T^* - ki_{qs}i_{ds} = 0\,. \tag{16}$$

The cost function is defined using the Kuhn-Tucker theorem

$$J(i_{ds}, i_{qs}) = W_{tot}(i_{ds}, i_{qs}) + \mu(ki_{qs}i_{ds} - T^*)\,, \tag{17}$$

where μ is a Lagrange multiplier.

The optimal solution is given, when

$$\frac{\partial J}{\partial i_{ds}} = \frac{\partial J}{\partial i_{qs}} = \frac{\partial J}{\partial \mu} = 0\,, \tag{18}$$

$$\begin{aligned} \frac{\partial J}{\partial i_{ds}} &= 2Ai_{ds} + \frac{Ci_{ds}}{\sqrt{i_{ds}^2 + i_{qs}^2}} + \mu k i_{qs} = 0\,, \\ \frac{\partial J}{\partial i_{qs}} &= 2Bi_{qs} + \frac{Ci_{qs}}{\sqrt{i_{ds}^2 + i_{qs}^2}} + \mu k i_{ds} = 0\,, \\ \frac{\partial J}{\partial \mu} &= ki_{ds}i_{qs} - T^* = 0 \end{aligned} \tag{19}$$

By combination of the above equations and after some manipulations, we can get

$$2\sqrt{i_{ds}^2 + i_{qs}^2}\left(Ai_{ds}^2 - Bi_{qs}^2\right) = C\left(i_{qs}^2 - i_{ds}^2\right). \tag{20}$$

The resolution of (20) is complex, using an alternative formulation in terms of instantaneous positions of the stator current and reference space vector with respect to the d-axis of the reference frame and using the inverter current constraint

$$i_{ds}^2 + i_{qs}^2 \le I_{\max}^2\,,$$

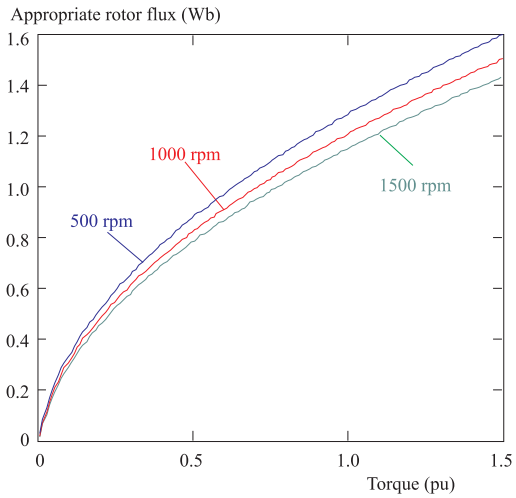

Fig. 2. Appropriate rotor flux versus torque.

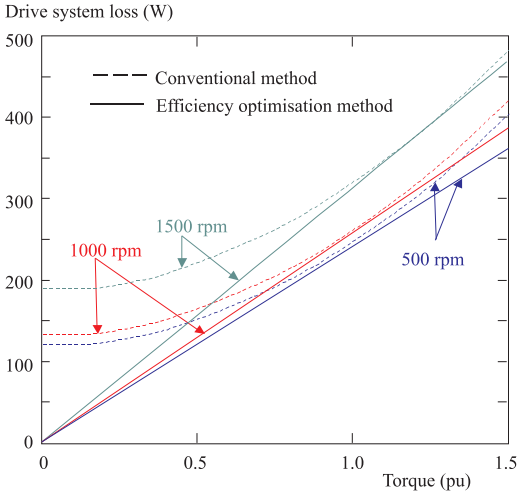

Fig. 3. Loss map of the drive system.

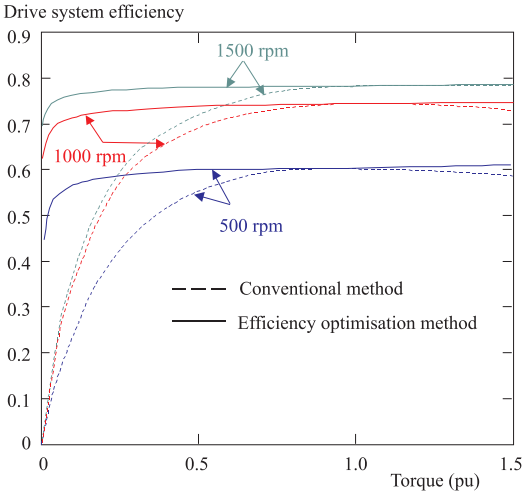

Fig. 4. Map of the efficiency.

where $I_{\max}$ is the boundary inverter current and in most cases equal to 1.5-times machine's current ratings. Then, stator d-q axis currents can be written as

$$i_{ds} = I_{\max}\cos\theta\,, \quad i_{qs} = I_{\max}\sin\theta\,. \tag{21}$$

Substituting (21) into (20) we can obtain the appropriate currents pair providing the minimum loss of the drive system:

$$\begin{aligned} i_{ds}^{*} &= \frac{I_{\max}}{2}\sqrt{\frac{C+2BI_{\max}}{C+(A+B)I_{\max}}} = \alpha\sqrt{|T^{*}|}\,, \\ i_{qs}^{*} &= \frac{I_{\max}}{2}\sqrt{\frac{C+2AI_{\max}}{C+(A+B)I_{\max}}} = \beta\sqrt{|T^{*}|}\,. \end{aligned} \tag{22}$$

Here

$$\alpha = \sqrt{\frac{K_{opt}}{k}}\,,\ \beta = \frac{1}{\sqrt{k\,K_{opt}}}\,,\ K_{opt} = \sqrt{\frac{C+2B(\omega_s)I_{\max}}{C+2A(\omega_s)I_{\max}}}.$$

The optimal rotor flux corresponding to the point of maximum efficiency at the steady state is then given by

$$\phi_r^{*} = L_m\alpha(\omega_s)\sqrt{|T^{*}|}\,. \tag{23}$$

The appropriate rotor flux given in (23) is plotted in Fig. 2. It is affected by the load torque and motor speed variations because core loss and stray load loss are taken into account. The rotor flux decreases so as to reduce the core loss and stray load loss, which increases with frequency than other loss at high speeds.

Figure 3 depicts the total loss of the drive system (including inverter loss) for both conventional method and efficiency optimization method. One can see that the total power loss for the proposed method is lower than that for the conventional method, which keeps the rotor flux level constant at its rated value. Figure 4 shows an efficiency map versus torque. It is clear that the proposed method is superior over a wide range of torques.

3 EXTENDED PREDICTIVE CONTROL CASCADE ECGPC/MRM

To overcome to the limitations of traditional cascaded CGPC method [15–17] (which gives the possibility to control only two different variables simultaneously without saving energy in electrical machines), we propose a new extended predictive cascade structure to control position, speed and rotor flux at the same time (with possible extension to control the direct component of stator current) under energy saving control of the drive system. The scheme of Fig. 5 implies the definition of three GPC algorithms and consequently the minimization of three quadratic cost functions. The external loop (position loop) uses a simple GPC controller and the inner loops (velocity and rotor flux loops) use a GPC/MRM with multiple reference models to follow specified trajectories.

The plants to be controlled assume the Controlled Auto Regressive Integrated Moving Average model (CARIMA) form, with dead-time equal to one:

$$A\big(q^{-1}\big)y(t) = q^{-1}B\big(q^{-1}\big)u(t) + \frac{C(q^{-1})}{\Delta(q^{-1})}\xi(t) \tag{24}$$

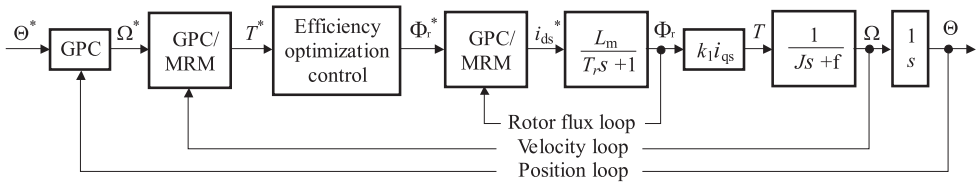

Fig. 5. Extended cascaded predictive structure ECGPC/MRM of an induction motor with efficiency optimization control.

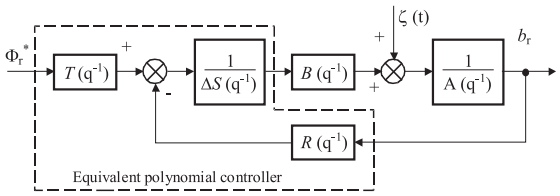

Fig. 6. GPC Equivalent polynomial RST controller.

where $u(t)$, $y(t)$ are input and output of the plant at the sample instance t, $\xi(t)$ is an uncorrelated random sequence and the use of the operator $\Delta\big(q^{-1}\big)= 1 - q^{-1}$ ensures an integral control law.
$A\big(q^{-1}\big)$, $B\big(q^{-1}\big)$, $C\big(q^{-1}\big)$, are polynomials in the backward shift operator q^{-1} and in most cases $C\big(q^{-1}\big)= 1$.

$$\begin{aligned} A\big(q^{-1}\big) &= 1 + a_1 q^{-1} + \cdots + a_{na} q^{-na}\,, \\ B\big(q^{-1}\big) &= b_0 + b_1 q^{-1} + \cdots + b_{nb} q^{-nb}\,. \end{aligned} \tag{25}$$

The main advantage of GPC/MRM structure is that the tracking model chosen by the designer ensures asymptotic behaviour input-output, so that

$$A_r\big(q^{-1}\big) y_r = q^{-1} B_r\big(q^{-1}\big) w(t) \tag{26}$$

where $B_r\big(q^{-1}\big)= B\big(q^{-1}\big)P\big(q^{-1}\big)$, $P\big(q^{-1}\big)$ is assigned in order to ensure the static behaviour $y_r(\infty) = w(\infty)$, and $A_r\big(q^{-1}\big)$ is specified to obtain good dynamic performance. The reference control signal $u_r(t)$ introduced by E. Irving [14, 17] is defined by

$$A\big(q^{-1}\big) y_r(t) = q^{-1} B\big(q^{-1}\big) u_r(t)\,. \tag{27}$$

Relation (27) can be rewritten as

$$A_r\big(q^{-1}\big) u_r(t) = A\big(q^{-1}\big) P\big(q^{-1}\big) w(t)\,. \tag{28}$$

The objective is to minimize multi-stage cost functions involving pseudo-tracking errors and control weighting terms.

$$\begin{aligned} J_{GPC} &= \sum_{N_{11}}^{N_{21}} \varepsilon_{y1}^2 + \lambda_1 \sum_{N_{11}}^{N_{u1}} [\Delta u_1(t+j-1)]^2, \\ J_{GPC1/MRM} &= \sum_{N_{12}}^{N_{22}} [\varepsilon_{y2}(t+j)]^2 + \lambda_2 \sum_{N_{12}}^{N_{u2}} \varepsilon_{u2}^2(t+j-1), \\ J_{GPC2/MRM} &= \sum_{N_{13}}^{N_{23}} [\varepsilon_{y3}(t+j)]^2 + \lambda_3 \sum_{N_{13}}^{N_{u3}} \varepsilon_{u3}^2(t+j-1), \end{aligned} \tag{29}$$

where

$$\begin{aligned} \varepsilon_{y1}(t+j) &= \hat{y}_1(t+j) - y_1^*(t+j), \\ \varepsilon_{y2}(t+j) &= \hat{y}_2(t+j) - \hat{y}_{2r}(t+j), \\ \varepsilon_{y3}(t+j) &= \hat{y}_3(t+j) - \hat{y}_{3r}(t+j), \\ \varepsilon_{u2}(t+j) &= \Delta\hat{u}_2(t+j) - \Delta\hat{u}_{2r}(t+j), \\ \varepsilon_{u3}(t+j) &= \Delta\hat{u}_3(t+j) - \Delta\hat{u}_{3r}(t+j). \end{aligned}$$

$$\begin{aligned} &\Delta u_1(t+j) \equiv 0 \text{ for } j \geq N_{u1}, \\ \text{Subject to:}\quad &\varepsilon_{u2}(t+j) \equiv 0 \text{ for } j \geq N_{u2}, \\ &\varepsilon_{u3}(t+j) \equiv 0 \text{ for } j \geq N_{u3}. \end{aligned} \tag{30}$$

The resolution must be down as follows:

- First, the minimization of J_{GPC} will provide the speed setpoint that must be followed by the rotor speed.
- Then, the minimization of $J_{GPC1/MRM}$ gives the reference torque which will provide via the efficiency optimisation control law the rotor flux setpoint.
- Finally, the cost function $J_{GPC2/MRM}$ will be minimized, providing the global command of the chain which is the direct component of stator current.

The minimization of J_{GPC} and $J_{GPC1/MRM}$ has been presented for CGPC structure in previous studies [17], here we have to present only the minimization of $J_{GPC2/MRM}$.

The transfer function between the estimated rotor flux and the flux current component i_{ds} in continuous plane can be given as

$$\frac{\phi_r(s)}{i_{ds}^*(s)} = \frac{L_m}{T_r s + 1}\,. \tag{31}$$

The Z-transform of the process transfer function (31) can be derived as

$$\frac{\phi_r\big(q^{-1}\big)}{i_{ds}^*\big(q^{-1}\big)} = \frac{q^{-1} B\big(q^{-1}\big)}{A\big(q^{-1}\big)}\,. \tag{32}$$

Then, identification of the process is performed using a recursive least square RLS estimator providing the unknown parameters $(a_1, \ldots, a_{na}, b_1, \ldots, b_{nb})$.

The previous CARIMA model is now used to elaborate the predicted outputs under the form

$$\hat{\varepsilon}_{y3}(t+j) = \underbrace{G_j\big(q^{-1}\big)\varepsilon_{u3}(t+j-1)}_{\text{Forced response}} + \underbrace{F_j\big(q^{-1}\big)\varepsilon_{y3}(t) + H_j\big(q^{-1}\big)\varepsilon_{u3}(t-1)}_{\text{Free response}}, \tag{33}$$

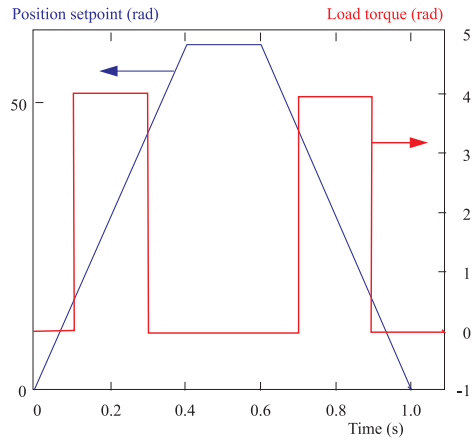

Fig. 7. Position setpoint and load torque trajectories.

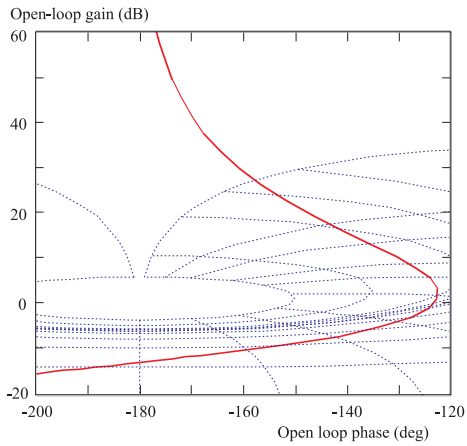

Fig. 8. Nichols diagram of the position loop.

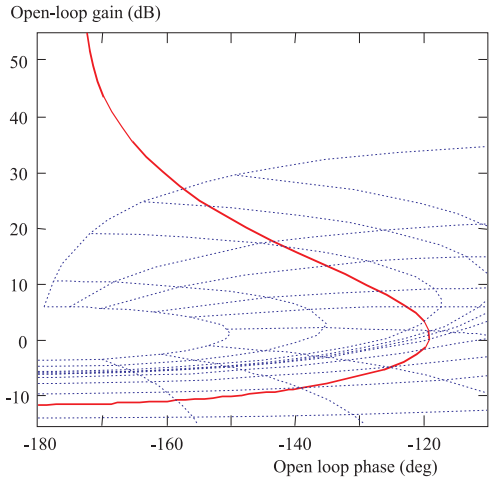

Fig. 9. Nichols diagram of the velocity loop.

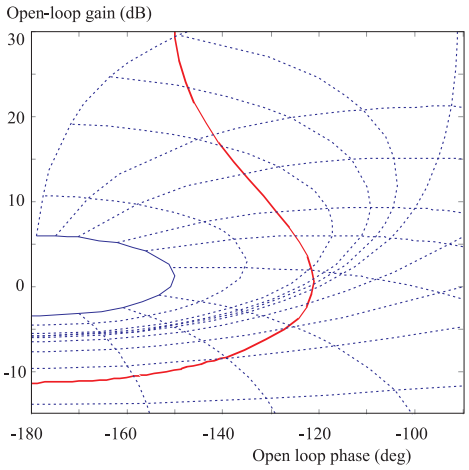

Fig. 10. Nichols diagram of the rotor flux loop.

where F_j, G_j, H_j are polynomials obtained by solving Diophantine equations, so that

$$\hat{\varepsilon}_{y3} = \mathbf{G}\varepsilon_{u3} + \mathbf{F}\,, \tag{34}$$

where

$$\mathbf{G} = \begin{bmatrix} g_{N_{13}}^{N_{13}} & g_{N_{13}}^{N_{13}} & \cdots \\ g_{N_{13}+1}^{N_{13}+1} & g_{N_{23}-1}^{N_{23}} & \cdots \\ \cdots & \cdots & \cdots \\ g_{N_{23}}^{N_{23}} & g_{N_{23}-1}^{N_{23}} & \cdots \; g_{N_{23}-N_{u3}+1}^{N_{23}} \end{bmatrix} \tag{35}$$

Minimization of $J_{GPC2/MRM}$ gives the optimal control values $\tilde{\varepsilon}_{u3}$,

$$\frac{\partial J_{GPC2/MRM}}{\partial \hat{\varepsilon}_{u3}} = 0 \tag{36}$$

$$\boldsymbol{\varepsilon}_{u3\,opt} = -\mathbf{M}[\mathbf{F}\varepsilon_{y3}(t) + \mathbf{H}\varepsilon_{u3}(t-1)] \tag{37}$$

where $\mathbf{M} = [\,G^{\top} \quad G + \lambda_3 I_{N_{u3}}\,]^{-1}$,
$G^{\top} = [\,M_1 \quad M_2 \quad \ldots \quad M_{N_{u3}}\,]^{\top}$ have to be computed off line, only the first control value of the sequence is applied on the system, so that

$$u_{3opt}(t) = u_{3opt}(t-1) + \Delta u_{3r}(t) - M_1\big[\mathbf{F}\varepsilon_{y3}(t) + \mathbf{H}\varepsilon_{u3}(t-1)\big]. \tag{38}$$

The procedure is repeated for the next sample intervals likewise.

4 STABILITY ANALYSIS

The advantage of RST polynomial structure is that these modules can be computed off-line, providing a very short real-time loop and on the other hand offers the possibility to analyze the stability of the controlled open loop in the frequency domain. In fact, this off-line operation is a very helpful strategy to determine the stable set of tuning parameters just before applying the control law on the real system. The RST polynomial form can be synthesized as shown by Fig. 6.

The polynomials RST can be identified by

$$\begin{aligned} R(q^{-1}) &= M_1\mathbf{F}\,, \\ S(q^{-1}) &= 1 + q^{-1}M_1\mathbf{H}\,, \\ T(q^{-1}) &= M_1\big[q^{13} \ \ldots \ q^{23}\big]\,. \end{aligned} \tag{39}$$

The GPC controller under polynomial form requires tuning of the set parameters N_1, N_2, N_u and λ to

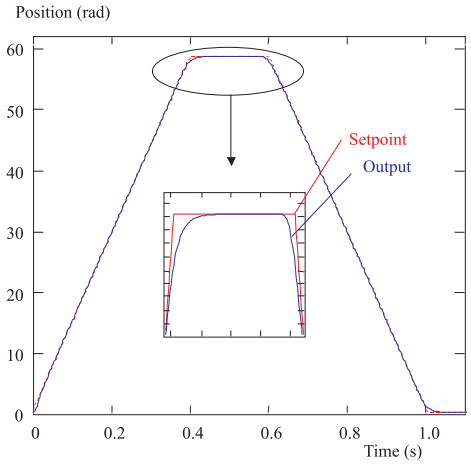

Fig. 11. Position output.

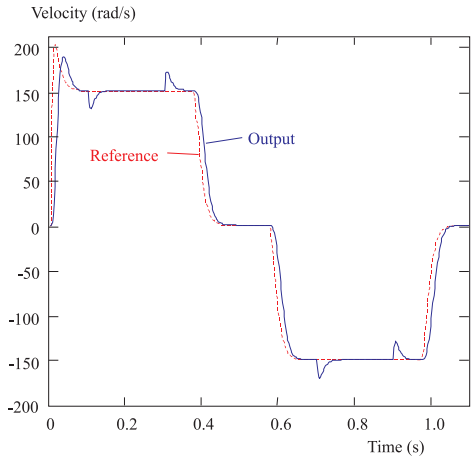

Fig. 12. Rotor speed.

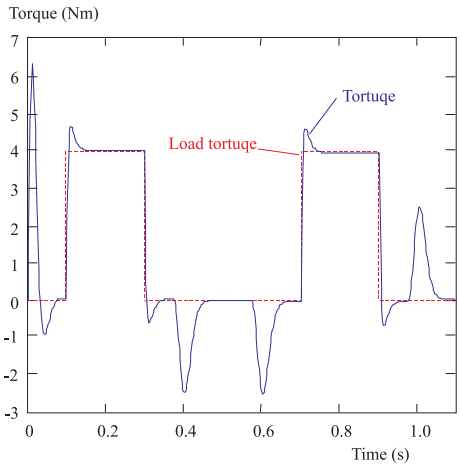

Fig. 13. Torque.

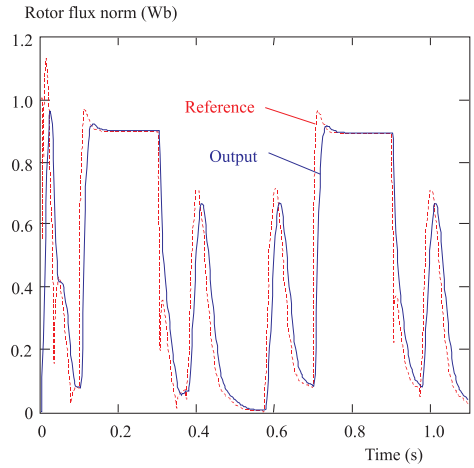

Fig. 14. Rotor flux norm.

ensure good stability. Some guidelines may be found in the literature [17].

$$N_1 = \frac{\text{dead-time of the system}}{\text{sampling period}} = 1\,,$$
$$N_2 \leq \frac{\text{response time of the system}}{\text{sampling period}}\,, \tag{40}$$

very often N_u is chosen so that $N_u << N_2$ and the case $N_u = 1$ is very interesting,

$$\lambda_{opt} = \mathrm{tr}\left(G^{\top} G\right).$$

5 SIMULATION RESULTS AND DISCUSSION

The system performance is examined by extensive simulation computer under different conditions such as motor speed and load torque variations. The drive system nameplate data and parameters are shown in the Appendix. The chosen example of motor position reference and load torque trajectories is given by Fig. 7. The position setpoint is a trapezium producing variations of the speed about 150 rd/s. The motor initially operates under no-load conditions, at $t = 0.1$ s, the load torque is stepped to 4 Nm in order to examine the impact of the load condition on efficiency optimization control and robustness regulation performance.

The set of parameters $[N_1,\, N_2,\, N_u,\, \lambda]$ providing good stability that has been chosen for the three open controlled loops and all the results about phase and gain margins GP, GM and bandwidth W_c are summarized in Table 1.

Table 1. Chosen parameters with frequency characteristics of the open controlled loops.

	N_1	N_2	λ	N_u	GM(dB)	$GP(^\circ)$	W_c(rd/s)
Position loop	1	13	0.0029	1	12.85	56.74	226
Velocity loop	1	10	4358.2	1	11.36	60.9	278.6
Flux loop	1	8	0.0065	1	11.31	58.8	286.4

The following diagrams show the frequency responses of the open controlled loop in the Nichols plane, Fig. 8 for position loop, Fig. 9 for velocity loop, and Fig. 10 for rotor flux loop.

In Figs. 11 and 12, the specifications are no overshoot for the position, and the tracking model for the velocity

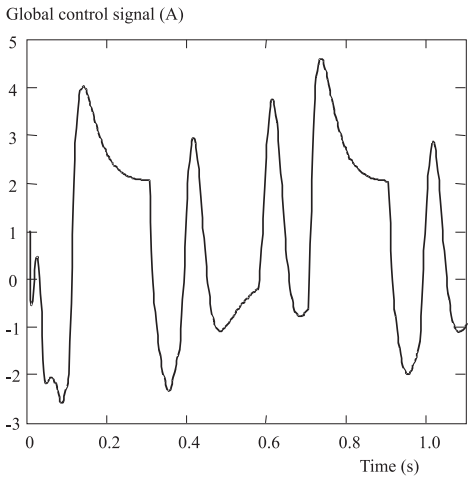

Fig. 15. Global control signal.

is: $\zeta = 0.707$, $\omega_0 = 120$ rd/s. It is clear that the position and speed outputs tracks their reference values with good dynamic performance (time response, cancellation of disturbances, ...).

Figure 13 shows the electromagnetic torque reference signal. It is easier to see that the torque follows the load torque variations in the steady state. Figures 14 and 15 illustrate both the rotor flux response and the global control signal (direct component of stator current). The tracking model for the rotor flux is: $\zeta = 1$, $\omega_0 = 60$ rd/s and it is easy to see that the rotor flux follows the load torque and speed variations as it is given by relation (23). These results demonstrate that the proposed method saves more energy without degradation in torque response than conventional methods.

6 CONCLUSIONS

In this paper, a new ECGPC/MRM of an induction motor drive under efficiency optimization control is presented to overcome the limitations of traditional CGPC. The ECGPC makes possible to control simultaneously more variables than conventional CGPC method and saves more energy of the induction motor drive. The control signal has been synthesized under the RST form which offers the possibility to analyze the stability of the controlled open loops in the frequency domain. The obtained performances have provided the effectiveness of the design and the stability of the system is ensured by a proper choice of the tuning parameters. Based on extensive simulations, the ECGPC/MRM with efficiency optimization control appears to be a useful method, well adapted for large application of drive systems.

Appendix

1.1 kW, 1500 rpm, 3.5 A, 220/380 V, 1.14 Wb, 7 Nm, $R_s = 8.1$, $R_r = 3.2$, $L_s = L_r = 0.48$ H, $L_m = 0.46$ H, inertia 0.006 (S.I).

References

[1] ABRAHAMSEN, F. *et al*: On the Energy Optimized Control of Standard and High Efficiency Induction Motors in CT and HVAC Applications, IEEE Trans. on Ind. Appl **34** No. 4 (1998).

[2] ABRAHAMSEN, F. *et al*: State of the Art of Optimal Efficiency Control of Low-Cost Induction Motor Drives, Proc. of PEMC'96, Budapest, Hungary, Sept. 1996, vol. 2, pp. 163–170.

[3] KIOSKERIDIS, I. *et al*: Loss Minimization in Scalar-Controlled Induction Motor Drives with Search Controllers, IEEE Trans. on Power Elec. **11** No. 2 (March 1996), 213–220.

[4] TANIGUCHI, S. *et al*: A Method of Speed Sensorless Control of Direct-Field-Oriented Induction Motor Operating at High Efficiency with Core Loss Consideration, Proc. of the IEEE/IECON' 2001.

[5] MENDES, E.*et al*: Losses Minimization of a Field Oriented Controlled Induction Machine, Proc. of the Electrical Machines and Drives Conf. pp. 310–314, 1995.

[6] CHAKRABOTRY, C. *et al*: Fast Efficiency Optimization Techniques for the Indirect Vector Controlled Induction Motors, IEEE Trans. on Ind. Appl. **39** No. 4 (2003).

[7] MATSUZE, K. *et al*: High Response Flux Control of Direct Field Oriented Induction Motor with High Efficiency Taking Core Loss into Account, IEEE Trans. on Ind. Appl. **35** No. 1 (January 1999).

[8] GARCIA, G. O. *et al*: An Efficient Controller for an Adjustable Speed Induction Motor Drive, IEEE Trans. on Ind. Electron. **41** No. 5 (1994), 533–539.

[9] LORENZ, R. D. *et al*: Efficiency-Optimized Flux Trajectories for Closed Cycle Operation of Field Orientation Induction Machine Drives, IEEE Trans. on Ind. Appl. **28** No. 3 (1992), 574–580.

[10] IEEE Standard Test Procedure for Polyphase Induction Motors and Generators, IEEE Std 112-1996.

[11] FERNANDEZ-BERNAL etal: Model Based Minimization for DC and AC Vector-Controlled Motors Including Core Saturation, IEEE Trans. On Ind. Appl. **36** No. 3 (2000), 755–763.

[12] CLARKE, D. W.—MOHTADI, C.—TUFFS, P. S.: Generalized Predictive Control — Part I. The basic algorithm, Part II. Extensions and Interpretations, Automatica **23** No. 2 (1987), 137–160.

[13] DEMIRCIOGLU, H.—CLARKE, D. W.: Generalized Predictive Control with End-Point State Weighting, IEE Proceedings-D **140** No. 4 (July 1993).

[14] UDUEHI, D. *et al*: A Generalized Predictive Control Benchmark for SISO Systems, Proc. of the 41st IEEE Conf. on Decision and Control, Las Vegas, USA, December 2002.

[15] HEDJAR, R. *et al*: Cascaded Nonlinear Predictive Control of Induction Motor, Proc. of the 2000 Int. Conf. On Cont. Appl. Alaska, USA, September 25-27, 2000.

[16] HENTABLI, V. *et al*: CGPC with Internal Model Structure: Application to Induction motor control, Proc. of the 1997 IEEE Conf. On Cont. Appl. Hartford, October 5-7, 1997.

[17] DUMUR, D.—BOUCHER, P.—RODER, J.: Design of an Open Architecture Structure for Implementation of Predictive Controllers for Motor Drives, Proc. of the 1998 IEEE Int. Conf. on Cont. App. pp. 1307–1311. Trieste, Italy 1-4 Sept. 1998.

Received 18 April 2006

Kamel Barra was born in Batna, Algeria in 1967. He received the Engineer and Master grades from Batna University, Algeria, in 1991 and 1999. He is currently working on his PhD thesis, all in electrical engineering. From 1999 until now, he has been with the Electrical Engineering Institute at Oum El Bouaghi University. His research interests are Power Electronics and intelligent control applied to Electrical machines.

Khier Benmahammed. Biography not supplied.